Journal of Materials and Engineering Structures

Research Paper

Numerical study of the effects of crown discharge on the separation bulbs of the leading edge with low Reynolds numbers

Wassila Guebli * , Djaffar Semmar, Koceila Mehalaine

Department of Engineering Mechanics, LApEH,Blida1University, Soumâa Road BP 270, 09000, Blida, Algeria

ARTICLE INFO

Article history:

Received : 22 August 2020

Revised : 19 June 2021

Accepted : 24 August 2021

Keywords:

Electro hydrodynamics

Corona Discharge

Plasma

Flow Control

ABSTRACT

Surface atmospheric plasmas can act on the boundary layer of a flow along a profile. Different types of plasma actuators are currently being studied in specialized laboratories. The objectives in the aerodynamic domain can be to control the laminar-turbulent transition, the decrease in drag, the increase in lift, the reduction of noise and consumption.

The object of this work is to use plasma actuators by characterizing their physical properties and their effects on flows. Two configurations were used: surface discharges with strip electrodes and wire electrodes. The ionic wind induced by these actuators is of low speed (a few m/s). This mechanical property was used to modify the boundary layer developing on a flat plate. The leading edge detachments from the profile flow have been delayed or even eliminated. The digital modeling and resolution of flow subjected to surface corona discharges, consists of a study based on the numerical simulation of the stationary behavior of a corona discharge in air at atmospheric pressure, carried out using the FLUENT software

1 Introduction

For several years, electric discharges established in air at atmospheric pressure have been used to control flows [1, 2]. In this case, the discharge is an integral part of a device called a plasma actuator. The plasma actuator consists in applying a potential difference between at least two electrodes placed on an aerodynamic surface [3]. Under the effect of the electric field, charged particles are generated in the flow and move at high speeds in the discharge interval, transfer the momentum to the neutrals and create an ionic wind over the dielectric surface. This phenomenon is used to modify the properties of the flow and bring it to the desired state. For example, the surface discharge produced by these devices is able to tangentially accelerate the flow field by means of the electro-hydrodynamic (EHD) interaction[4, 5]. In this article, we present a numerical study of a subsonic laminar flow under the effect of corona discharges generated on the surface of a flat dielectric plate having configurations of plasma actuators, strip electrodes and wire electrodes. The objective is not to

* *Corresponding author. Tel.: +213 655136798.*
E-mail address: guebliw@gmail.com

e-ISSN: 2170-127X,

RESEARCH REVIEW of Sciences and Technologies

model the plasma / flow interaction at the molecular level, but rather to determine the overall effect of an electric field on the flow. This approach has already been used to solve problems of electrostatic precipitators [6, 7]. Later, other studies[8, 9] used it to model the effects of corona discharges on the boundary layers of airflow, both in laminar and turbulent cases. The results show that this approach is very effective in describing the flow trends when subjected to plasma actuation. Consequently, the acceleration of the laminar boundary layers has been successfully simulated, as well as the drag reduction.

2 Modelling and numerical simulation

The simulation of electro-aerodynamic phenomena produced by corona discharge actuators requires a model taking into account both the physics of discharges and that of aerodynamics. In current research, it is not intended to model the interaction of ions and molecules at the molecular level, but rather to find the overall effect of an electric field on the airflow. The work presented consists of a study based on the numerical simulation of the stationary behaviour of a corona discharge in air at atmospheric pressure. The influence of the electric field on the flow is taken into account by adding an electric force term to the Navier-Stokes equations. The numerical simulation is carried out using the CFD code FLUENT 6.3, which uses the finite volume method. In this work, the choice is focused on two different configurations of electrodes, namely: The first configuration based on the work of Pierre Magnier [10], consists of thin adhesive copper strips 35 µm thick, 175 mm long and 25 mm wide. They are fixed on either side of the rounded leading edge of a flat plate as shown in Fig1.

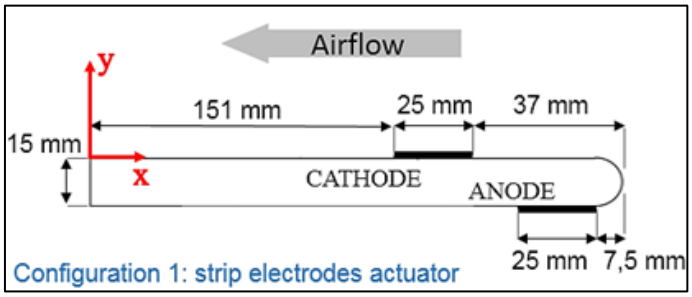

Fig. 1 –Configuration system for strip electrodes [10]

The second configuration studied is that used by E. Moreau [11] represented in Fig 2. Consists of a flat plate, with rounded leading edge and equipped with two thin wire electrodes placed inside grooves machined from an insulating material on the upper face. These two electrodes are connected to a high voltage power supply, which creates a corona discharge on the upper face of the flat plate, immersed in a flow of air.

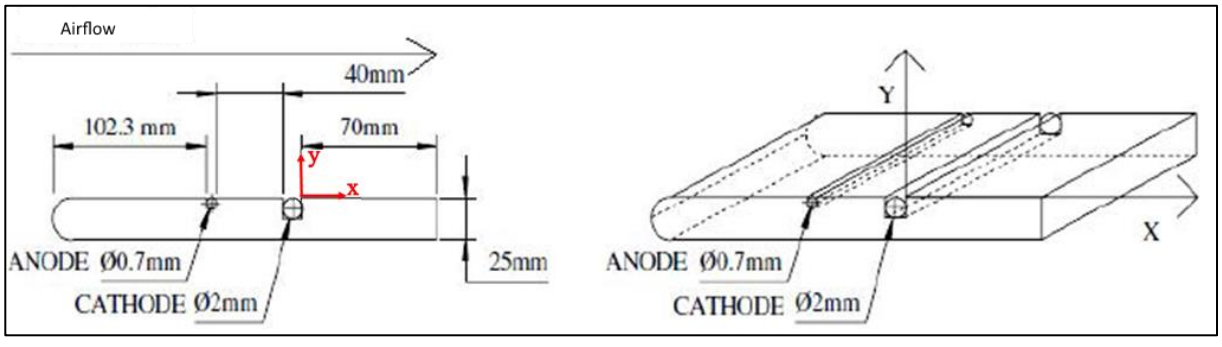

Fig.2 – Wired electrode configuration system [11].

The plate is 50cm wide, 21.5cm long and 25mm thick. The electrodes are 40mm apart. The anode is a 0.7mm diameter copper wire placed 10 cm downstream from the leading edge, with a positive potential. The second electrode is the 2mm diameter cathode brought to a negative potential. The plate is exposed to an air velocity of 5 m / s.

2.1 Numerical modeling

The numerical calculation was done using the CFD code Fluent 6.3, which uses the finite volume method as a discretization process. The integral equations that govern the flow, such that the continuity equation, the mass conservation equation, the energy and other scalars, such as turbulence, are solved by this method. Using this technique based on a control volume, Fluent goes through the following steps:

- Division of the domain into discrete control volumes using a computational grid (mesh)
- Integration of the governing equations on the individual control volumes, in order to construct the algebraic equations for the dependent discrete variables (the unknowns), such as velocities, pressure, etc.
- Linearization of the discretized equations and resolution of the resulting system of linear equations, in order to be able to update the values of the dependent variables (unknown).

2.2 Field of study and boundary conditions

The objective of the numerical simulation is using math equations to model the airflow, the electric field induced by the electric discharge process and the interaction between the two. The effect of the different parameters governing the electric field will be studied. The coupled system of equations will be solved to calculate the electric force that applies to the fluid.

We calculate a two-dimensional flow for the laminar regime on the flat plate with support for electrical forces. The area of calculation is divided into two areas. The first zone is that of the far field, while the second is the inter-electrode zone. For the configuration of the wire electrodes, it is modeled by a parallelepiped whose leading edges favor the flow as shown in Fig 3. A length of 4cm and a height h of 1.5mm characterizes this space. The same steps are followed for the configuration of the strip electrode. The surface corona discharge established induces a flow by the movement of the ions in the inter-electrode space. As these move near the wall of the anode towards the cathode, they bypass the circular geometry of the leading edge of the flat plate.

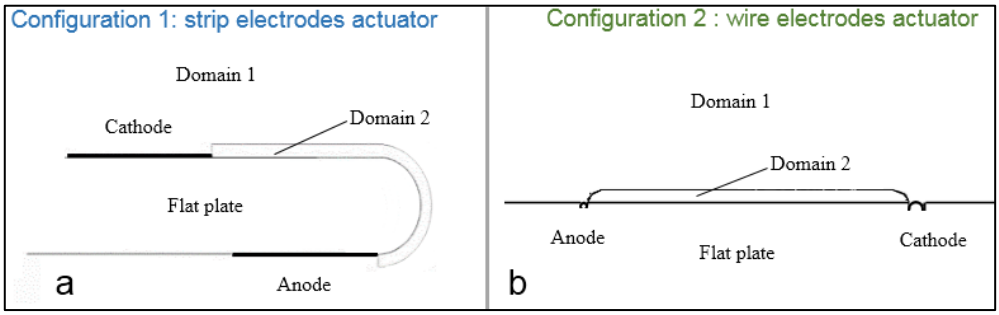

Fig. 3 – (a) Computational domains of the strip electrodes configuration, (b) the wire electrodes configuration

The boundary conditions are a condition of adhesion to the wall, and a condition of sliding on the border.

2.3 Equations

For both configurations, the model developed is based on the following assumptions:

- Two-dimensional, stationary and incompressible flow.
- Only the coulomb force is present.
- The diffusion of ions is negligible.
- The electrical conduction coefficient does not depend on the electric field.
- The mobility of the ions is constant and independent of the intensity of the electric field.

In addition to the above assumptions, we need to determine the flow regime.

The system consists of the equations of fluid mechanics and those of electrostatics. In electricity, Coulomb proposed a similar law concerning the force of attraction or repulsion between two electric charges. Ions are subjected to a Coulomb Force F such as:

$$F = \rho_c E \tag{1}$$

with: ρ_c the charge density in (C.m^{-3}) and E : the electric field in (V/m).

The ions are directed towards the walls and collide with the molecules of fluid, which transfer a movement to these. It is equivalent to a force, which acts directly on the fluid, then the Navier-Stokes equations of incompressible flow field in dimensional terms are:

1- The continuity equation:

$$\frac{\partial u_i}{\partial x_i} = 0 \tag{2}$$

2- The equation of the conservation of momentum:

$$\rho\left[\frac{\partial u_i}{\partial t} + u_j \frac{\partial u_i}{\partial x_j}\right] = -\frac{\partial p}{\partial x_i} + \mu \frac{\partial^2 u_i}{\partial x_j^2} + F_i \tag{3}$$

with ρ : the density of the fluid in (Kg/m^3), p : the pressure in (Pa), μ : The dynamic viscosity in (Kg/m.s), u_i : speed field, x_i : Cartesian coordinates, F_i :coulomb force field.

The electrostatic equations:The distribution of the electrostatic potential and the distribution of the charge in space are given by the Maxwell equations:

$$\frac{\partial^2 V}{\partial x_i^2} = -\frac{\rho_c}{\varepsilon_o} \tag{4}$$

Such as

$$\rho_c^2 = \varepsilon_o \frac{\partial \rho_c}{\partial x_i}\frac{\partial V}{\partial x_i} = \varepsilon_o \frac{\partial \rho_c}{\partial x_i} E_i \tag{5}$$

with: $\varepsilon_o = 8.854 \times 10^{-12}$ the permittivity of the air, V :scalar electric potential.

Therefore, the electric field E derives from the scalar electric potential V :

$$E_i = -\frac{\partial V}{\partial x_i} \tag{6}$$

We have the expression of the current density J that shows the three transfer modes: conduction, convection and diffusion:

$$J_i = \rho_c \beta E_i + U\rho_c - D\nabla\rho_c \tag{7}$$

with: D is the coefficient of diffusivity of ions in (m²/s) and $\beta = 1.4311\times10^{-4}$ m s^{-1}(V m^{-1})$^{-1}$)is the mobility of the ions.

The equation of conservation of the electric charge should be added:

$$\frac{\partial J_i}{\partial x_i} = 0 \tag{8}$$

Taking into account the definition of electric potential (6) and the continuity equation (2), and substituting the expression for the current density (7) in (8) equation, we can obtain the equation of the following charge:

$$\frac{\partial}{\partial x_i}\left(-D\nabla\rho_c-\beta\rho_c\left(\frac{\partial V}{\partial x_i}\right)\right)+U\frac{\partial\rho_c}{\partial x_i}=0 \tag{9}$$

For a system, which describes the airflow in an induced ring, the term conduction in equation (7) is dominant before the terms of convection and diffusion. These terms are often overlooked in numerical simulations. We then obtain the following simplified equation:

$$\frac{\partial}{\partial x_i}\left(\beta\rho_c\left(\frac{\partial V}{\partial x_i}\right)\right)=0 \tag{10}$$

With the assumption that the charge density is constant in the inter-electrode zone, we find equation (4) in the form:

$$\frac{\partial}{\partial x_i}\left(\sigma\left(\frac{\partial V}{\partial x_i}\right)\right)=0 \tag{11}$$

where σ represents the electrical conductivity in (Sm^{-1}).

An important feature of this theoretical formulation of the problem is that the electrical equations can be solved independently of the equations governing the flow.

2.4 Numerical simulation

The influence of the electric field on the flow is taken into account by the addition in the Navier-Stokes equations of an electric force term. This approach does not explicitly take into account the presence of charged species in the electric field calculations. An additional UDF (User Defined Functions) calculation module is written in C language to calculate the electrostatic physical quantities necessary in equation (4) in order to simultaneously solve the electric potential and speed vector. This in turn allows for the effect of electrostatic forces on the equation of motion to be taken into account.

Finally, the mathematical model associated with domain 2 is as follows:

$$\begin{cases}\dfrac{\partial u_i}{\partial x_i}=0\\ \rho\left[\dfrac{\partial u_i}{\partial t}+u_j\dfrac{\partial u_i}{\partial x_j}\right]=-\dfrac{\partial p}{\partial x_i}+\mu\dfrac{\partial^2 u_i}{\partial x_j^2}+F_i\\ \dfrac{\partial^2 V}{\partial x_i^2}=0\\ E_i=-\dfrac{\partial V}{\partial x_i}\end{cases} \tag{12}$$

The mathematical model taking into account all the simplifying hypotheses for domain 1 is given by the following system:

$$\begin{cases}\dfrac{\partial u_i}{\partial x_i}=0\\ \rho\left[\dfrac{\partial u_i}{\partial t}+u_j\dfrac{\partial u_i}{\partial x_j}\right]=-\dfrac{\partial p}{\partial x_i}+\mu\dfrac{\partial^2 u_i}{\partial x_j^2}\\ \dfrac{\partial^2 V}{\partial x_i^2}=0\end{cases} \tag{13}$$

3 Results

The creation of the geometries as well as the mesh are done under the Gambit 2.3.16software. This software offers extended solutions for the most complicated geometries. Certain rules apply when building a mesh, in terms of cell size and shapes, to limit purely numerical errors. The mesh used and the calculation domain for this simulation are shown in Fig.4 and Fig.14. It is an unstructured mesh with triangular cells to ensure a minimum of digital diffusion.

3.1 The strip electrode actuator

By applying a voltage of about 40 kV, taking into account the height of the discharge zone h equal to 2 mm and different input speeds of 4m/s, 8m/s and 14m/s.

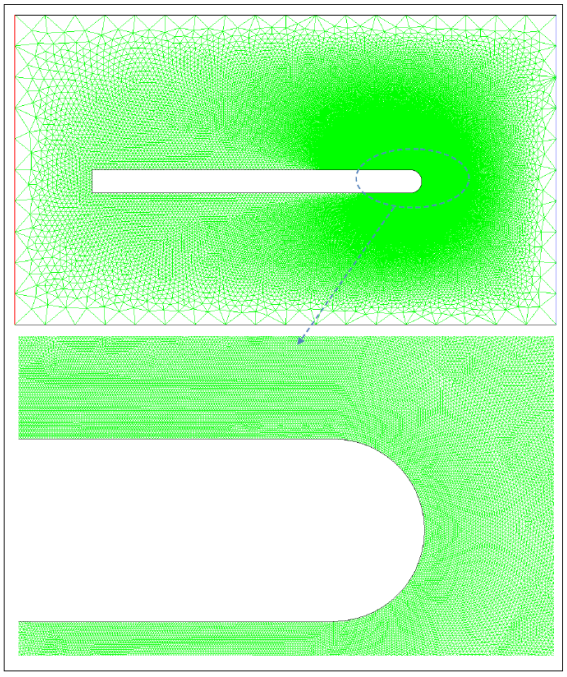

Fig. 4 – Meshing of the non-structured domain (92 233 nodes) configuration of strip electrodes

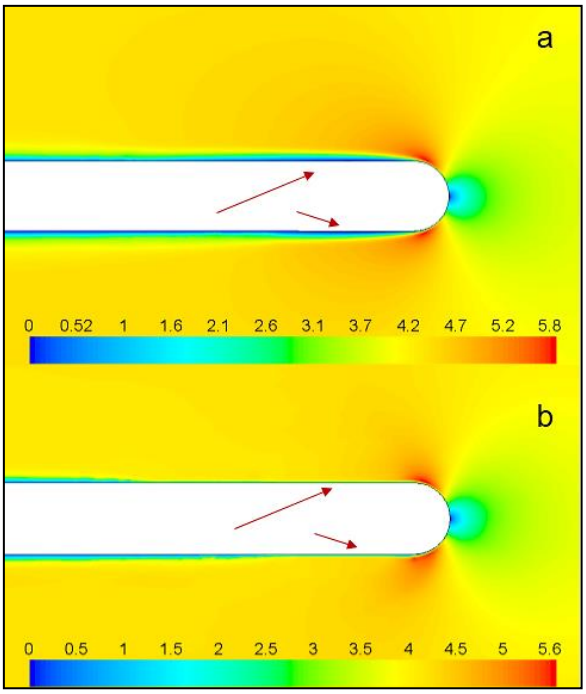

Fig. 5 – Velocity contours calculated for U = 4 m / s, without discharge (a), and with discharge, Difference in electrical potential ΔV = 40 kV (b).

Fig.5.a shows the distribution of flow around the leading edge region, a local separation is seen near the leading edge and the flow is well established between the anode and the cathode because the actuator is not activated yet. On the other hand, in Figure 5.b, the boundary layer is glued as if the flow were sucked in by the discharge, which bypasses the leading edge of the flat plate.

Fig. 6 clearly shows the acceleration of the flow in the inter-electrode zone in the presence of a discharge.

3.1.1 Effects of the actuator on the flat plate in incidence

The importance of the effect of the discharge on the flow is more or less great according to the type of flow regime. Thus, the discharge removes the small bulbs from the leading edge, while the larger bulbs are only reduced. For moderately separated flows, the detachment, which is due to the bursting of a leading edge bulb, is greatly reduced in the presence of the discharge.

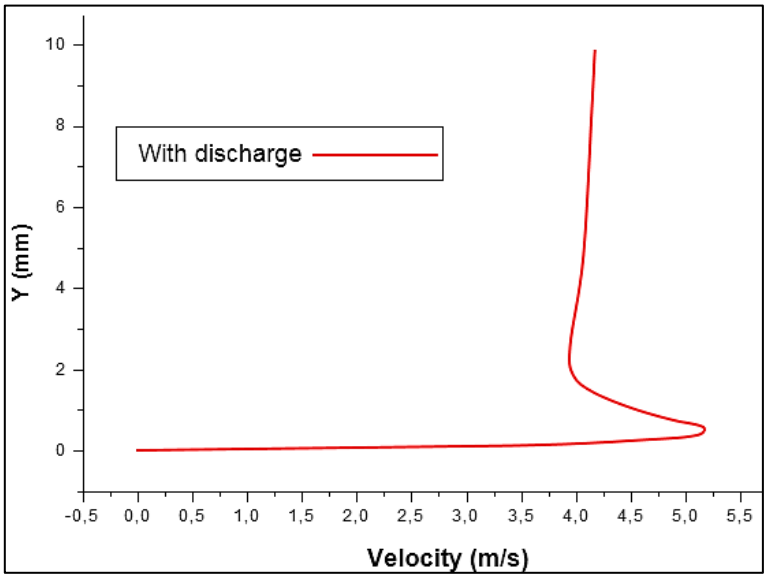

Fig. 6 – Computational boundary layer profile with discharge at 1 cm downstream the cathode, for Re = 5.83 104, Difference in electrical potential ΔV= 40 kV.

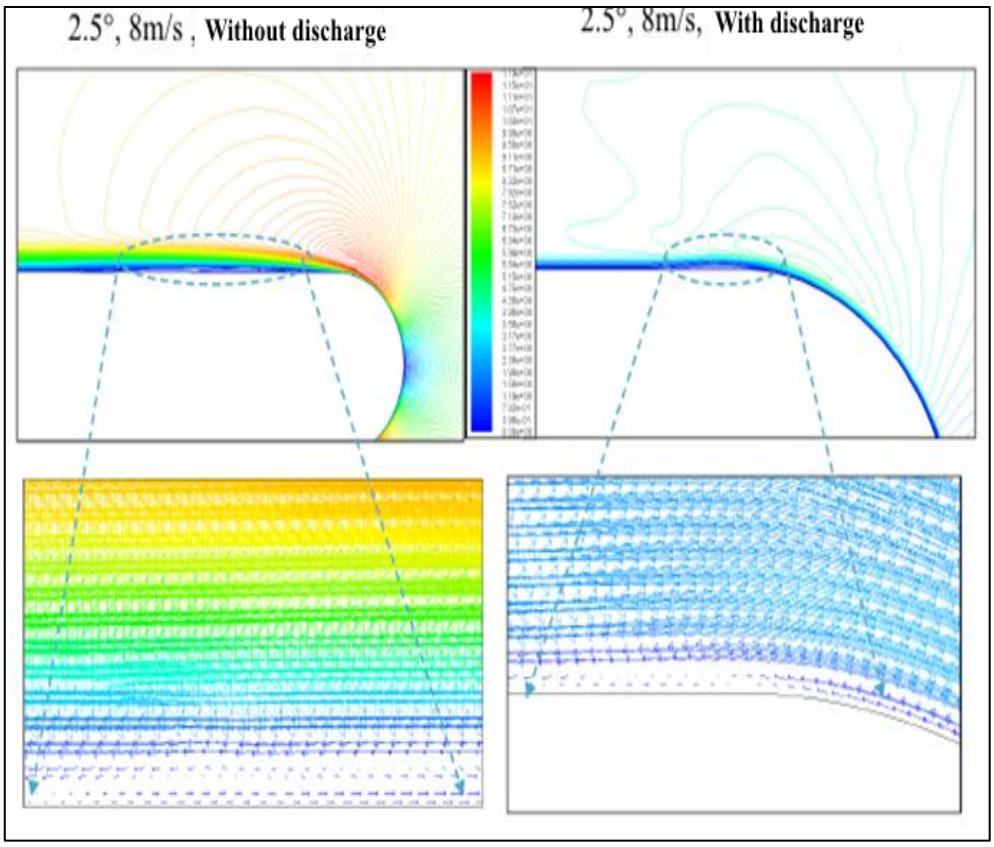

Fig.7– Velocity fields and streamlines with and without discharge for an angle of attack of 2.5 ° and a speed of 8m / s. (anode electrical potential Va = + 30kV and cathode electrical potentialVc = -10kV)

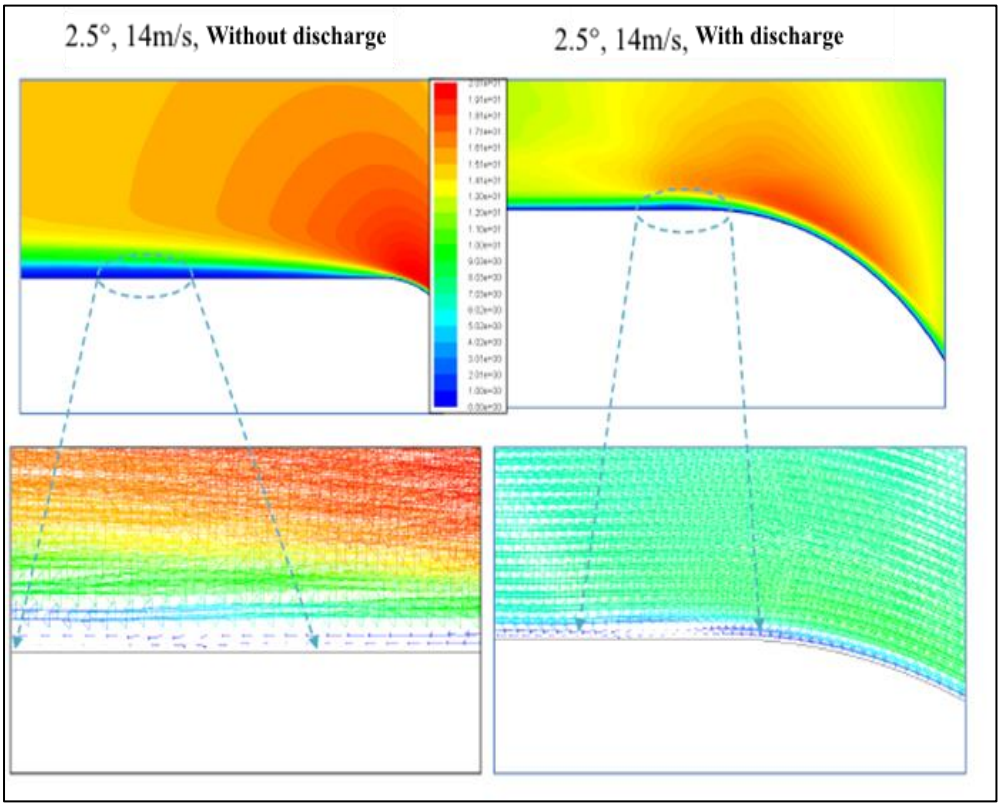

Fig.8 – Velocity fields and streamlines with and without discharge for an angle of attack of 2.5 ° and a speed of 14m / s. (Va = + 30kV and Vc = -10kV)

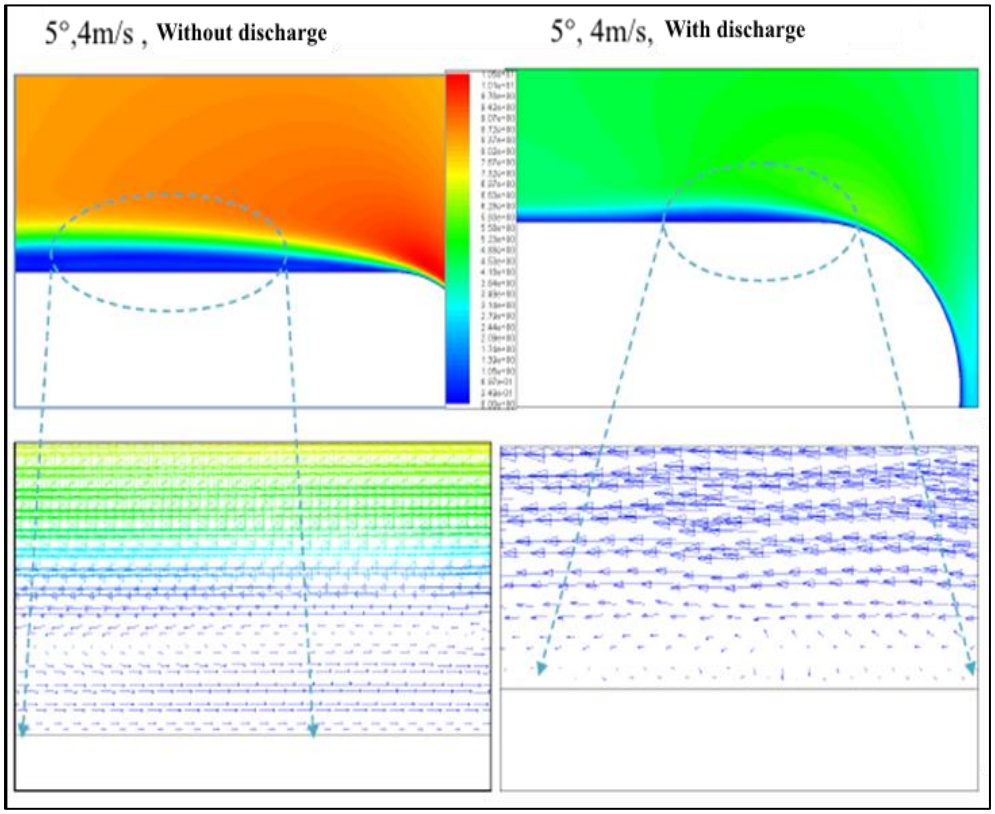

Fig. 9 – Velocity fields and streamlines with and without discharge for an angle of attack of 5 ° and a speed of 4m / s. (Va = + 30kV and Vc = -10kV).

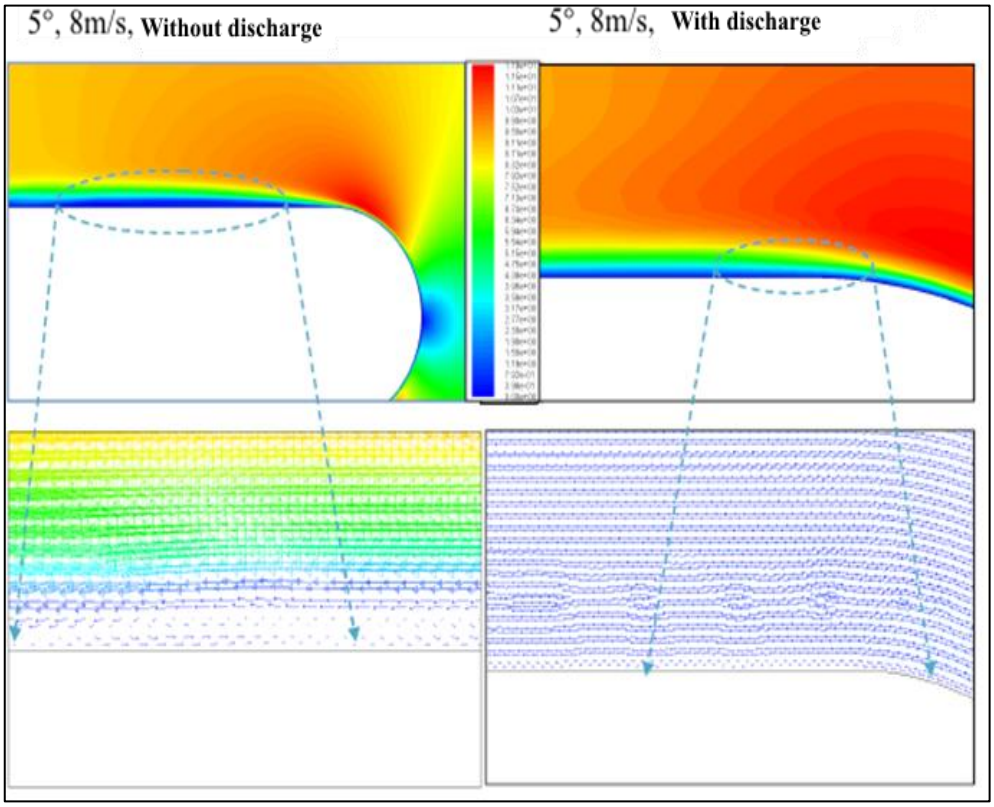

Fig. 10 – Velocity fields and streamlines with and without discharge for an angle of attack of 5 ° and a speed of 8m / s. (Va = + 30kV and Vc = -10kV).

3.1.2 Effects on the thickness of the boundary layer

From the speed profiles recorded before the cathode and behind the cathode for a constant discharge of 40kv and a speed of 4m / s,we were able to determine the thickness of the boundary layer when the speed reached 99% of the speed at infinity. Fig.11 shows the speed profiles obtained for different abscissae on the flat plate at zero incidence without and with electric discharge. These measurements allowed us to trace the thickness of the boundary layer without and with discharge and confirm the development of the boundary layer on the flat plate.

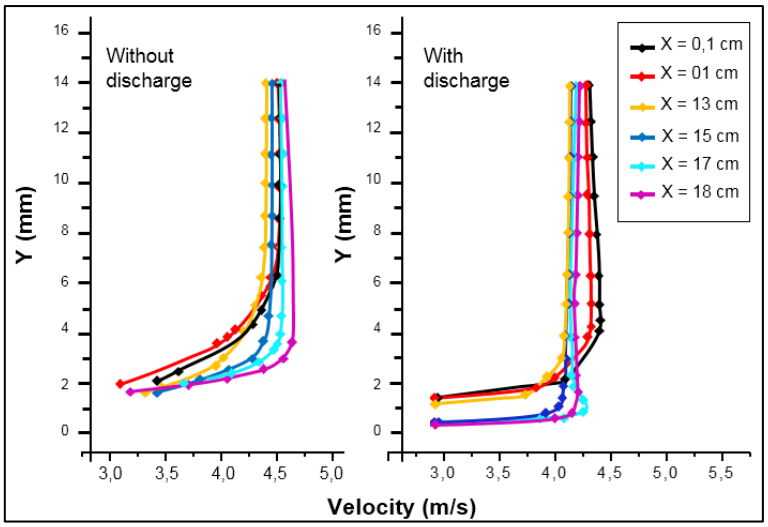

Fig. 11–Computational boundary layer profiles without discharge for R_e = 5.83 10^4 (left), and with discharge (right) when ΔV = 40 kV, at different positions on the plate.

Fig. 12 shows the variation in thickness of the boundary layer with and without discharge for a flow speed of 4 m / s.

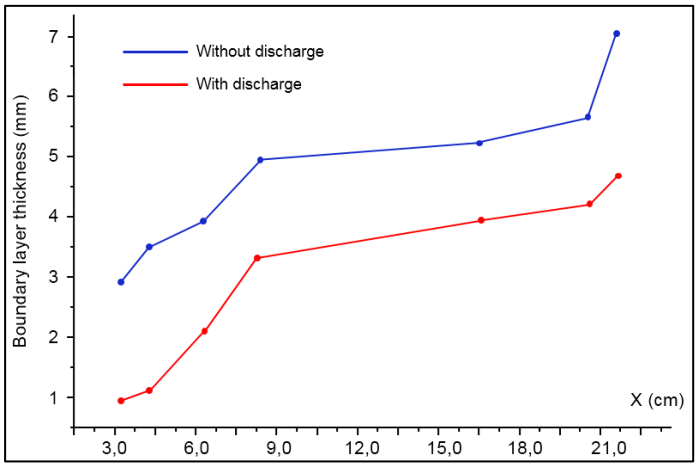

Fig. 12– Computational boundary layer thickness variation along the plates upper surface before, and after actuation for Re = 5.83 10^4, ΔV = 40 kV.

3.1.3 Effects on flat plate drag

The reduction of the bulbs and separation of the flow on the inclined flat plate by the corona discharge,results in a variation in the value of the forces applied to it.In the case of a flat plate with zero incidence, the drag of one face of the leading edge at a given x-coordinate can be determined from the speed profiles with the following formula [12]:

$$D(x) = b\rho \int_{y=0}^{\infty} u(U_0 - u)dy \tag{14}$$

with: b the width of the plate (here 30 cm), ρ the density of the air (kg.m^{-3}), u the local speed (m/s), U_0 the speed of the main flow (m/s).

The drag force applied to the flat plate at zero incidence and on the abscissa x = 40 mm downstream of the leading edge, is calculated for the three speeds 4m/s, 8m/s and 14m/s. For each flow velocity, the value of the drag is reduced by application of the discharge. For a speed of 14 m/s, it is reduced by 27.2%.

Indeed, by adding momentum close to the wall, the plasma actuator acts on the leading edge bulbs. Thus, the drag induced by this recirculation of fluid is greatly reduced by the reduction of the bulb.

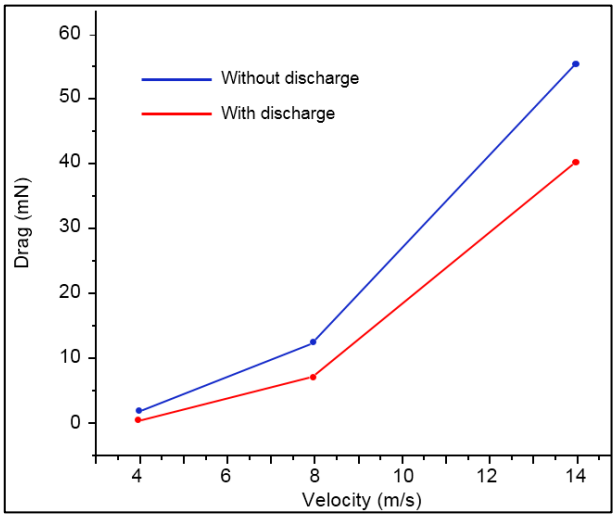

Fig. 13 – Computed Effect of 40 kV corona discharges on flat plate local drag at x = - 150 mm (or 40 mm downstream the leading edge)

This confirms the results on a flat plate obtained by Adamo et al. (2002) and Artana et al. (2000) (up to 34% reduction, up to 5 m / s) and confirms the results obtained by Pierre Magnier [10] in figure 14 (up to 17.6% reduction). We can see that there is a good agreement between the numerical and experimental results.

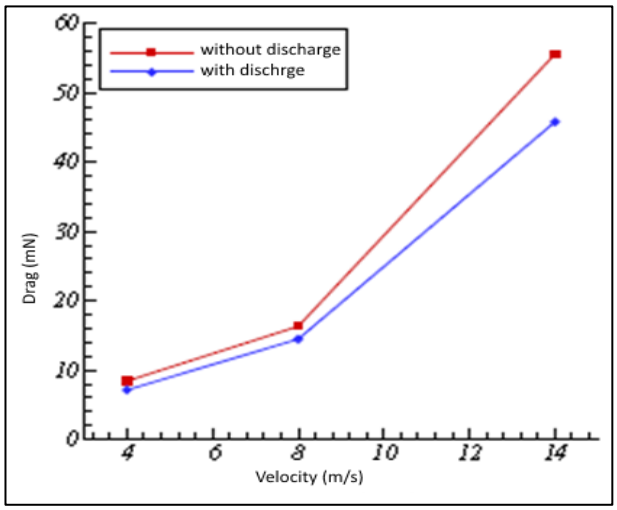

Fig. 14 –Experimental evolution of the drag on the flat plate of zero incidence, 40 mm downstream from the leading edge, as a function of the flow speed without and with discharge (current of 0.8 mA / m) [10].

3.2 The wired electrode actuator

We calculate a two-dimensional flow with a laminar regime on a flat plate at zero incidence. For that, one took an unstructured mesh of 69850 nodes fig.15. Calculations are made for several input speeds. Voltages of + 22kv are applied to the anode and -10kv to the cathode. For this calculation, we choose h, which represents the most active zone (the anode), produces ions over a radius of 1.5mm, i.e. the inter-electrode height [11-13]. Fig.15 and Fig.16 represent the speed iso-values along the profile considered for a speed of 5 m/s, without and with electric discharge respectively.

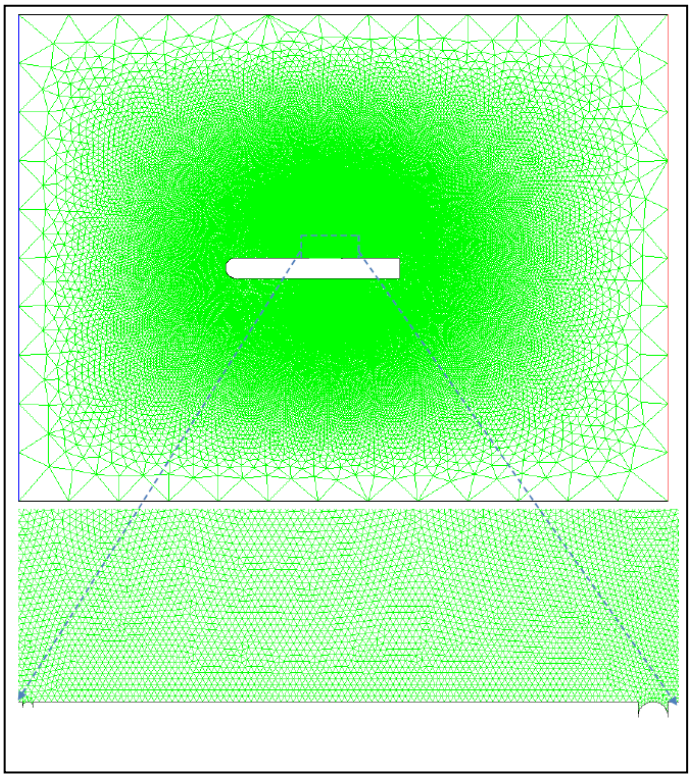

Fig.15 – Meshing of the non-structured domain (69,850 knots) of wired electrodes configuration

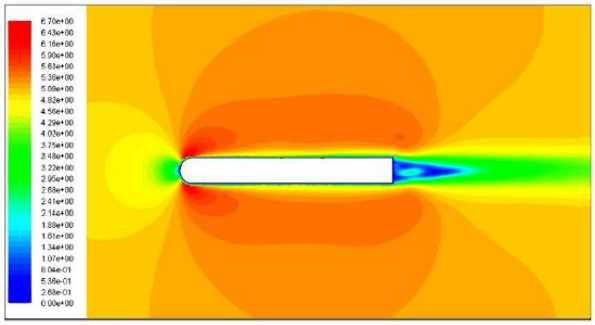

Fig. 16 –Velocity contours calculated without discharge with U = 5m / s

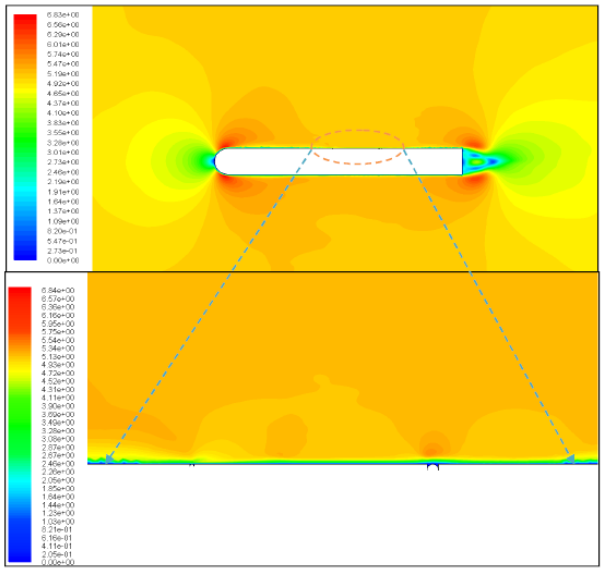

Fig.17 – Calculation speed contours with discharge at U = 5m / s, (Va = + 22kV and Vc = -10kV)

We can clearly see in Fig.16 the separation of the boundary layer on the upper surface in the absence of the discharge. The flow is well established in the inter-electrode area. While, in fig.17 there is a reattachment of the boundary layer in this zone. The simulations show that the application of an electrical potential of 32 kV to the wire electrodes changes the profiles of the boundary layer near the actuator Fig.18. It is also noted that the numerical results agree well with the experimental data of Moreau [11]. The flow in the boundary layer is accelerated by the impulse given by the electric discharge. This extra energy is injected into the first layers of the flow in the vicinity of the wall. Then it is diffused into the upper layers due to the viscosity. The boundary layer profile calculated at x = -12 mm (or 3 cm downstream of the anode) is also presented. These results suggest that the acceleration of the flow is greater in the discharge interval.

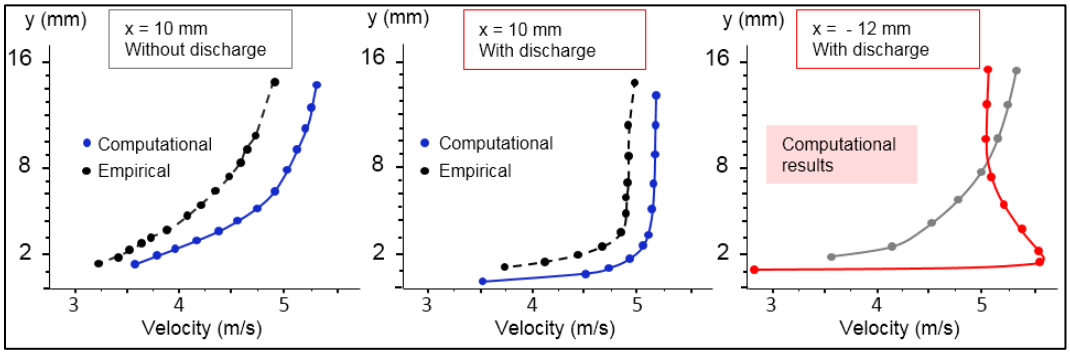

Fig.18– Comparison of boundary layer profiles with those of Moreau[11], before and after actuation at x = 10 mm (or 1 cm downstream of the cathode) and at x = -12 mm (or inter-electrode zone) for U = 5 m / s, ΔV = 32 kV

3.2.1 Effects on the leading edge separation bulb

From Fig.19, it can be seen that in the absence of the discharge, a medium-sized separation bulb develops near the leading edge of the flat plate for a speed of 5 m / s and an angle of incidence of 2.5 °. In the presence of the 32 kV corona discharge, Fig.19 shows almost the same results. The displacement of the electro-hydrodynamic wire actuator downstream of the leading edge certainly minimizes its effects on the separation of the flow. However, the reverse flow is significantly reduced even if the size of the separation bulb remains substantially the same in general.

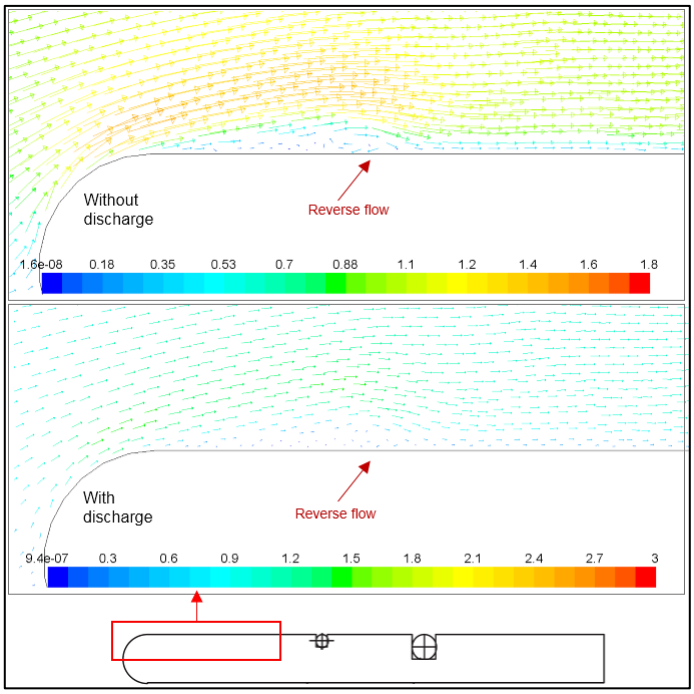

Fig.19 – Computational velocity vectors for U= 5 m/s, AOA = 2.5 ° ,without discharge (Up), with discharge ΔV = 32 kV (Down)

3.2.2 Effects on flat plate drag

In Fig.20, we can clearly see a reduction in the drag force at the trailing edge (x = 7cm) of up to 16.3%, without and with discharge for speeds of 5 to 25m / s. We also notice a strong resemblance between the results obtained and the experimental results of E. Moreau [11].

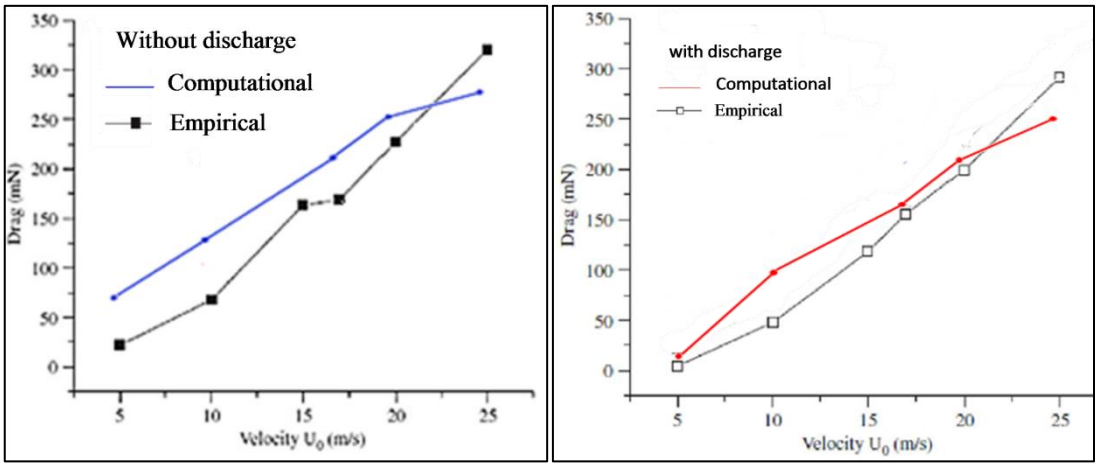

Fig.20 – comparison between the empirical results[11] and calculation of variation of the local drag of flat plate calculated as a function of air speed. Before and after actuation (ΔV = 40 kV).

4 Conclusion

In the current industrial context, reducing financial and energy costs is an essential objective of research programs in the transport industries. The optimization of aerodynamics and its control are part of this perspective. The study carried out during this article consists in developing plasma actuators, commonly called electro-hydrodynamic actuators, to modify subsonic flows.

Numerical simulations of the effects of crown discharges, produced by two actuator configurations, on a laminar flow with a flat plate are presented. The study relates to the hydrodynamic modifications of the boundary layer under the effect of plasma discharges as well as to the separation bulbs of the leading edge, namely, the thickness of the boundary layer and the drag.

The mathematical model used makes it possible to take into account the effect of discharges on the hydrodynamic flow, by introducing an appropriate acceleration force, without modeling the plasma itself. The calculation domain is divided into two regions for the two configurations. One represents the region of flow unaffected by discharges and the other the region where the effects of plasma are predominant. The differences between the two cases, with and without discharge, are clearly demonstrated, particularly in the area where the ionic wind generated by the crown discharges affects the flow.

In the first actuator configuration, the strip electrodes are placed very close to the leading edge of the plate. This actuator induces a low velocity relative to the main flow allows to act on the boundary layer by exciting instabilities and causing the laminar-turbulent transition. The importance of the effect of the discharge on the flow is greater or lesser depending on the type of flow regime. Thus, the discharge causes the small leading edge bulbs to disappear, while the larger bulbs are only reduced. Then in a second step, it was a question of validating its possibilities. In this case, the simulation results show a significant decrease in the drag of the plates, as well as the thickness of the boundary layer. It is also noted that this actuator is able to significantly reduce the size of the separation bulb.

The second actuator configuration consists of two wire electrodes housed in appropriate grooves on the top of the flat plate. The calculations show that the effect on the boundary layer and on the drag is essentially similar to the previous case. However, the effect on the flow separation bulb is minimal due to the position of the actuator away from the separation zone.

Considering what has been highlighted in this work, it would also be very interesting and useful to think about surface discharge configurations that could increase EHD force.

REFERENCES

[1]- J.A. Vernet, R. Örlü, P.H. Alfredsson, Flow separation control behind a cylindrical bump using dielectric-barrier-discharge vortex generator plasma actuators. J. Fluid Mech., 835 (2017) 852-879. doi:10.1017/jfm.2017.773.

[2]- T. Brauner, S. Laizet, N. Benard, E. Moreau, Modelling of Dielectric Barrier Discharge Plasma Actuators for Direct Numerical Simulations, in 8th AIAA Flow Control Conference: Washington, D.C. (2016). doi:10.2514/6.2016-3774.

[3]- L. Dong, G. Gao, K. Peng, W. Wei, C. Li, G. Wu, Effects of surface dielectric barrier discharge on aerodynamic characteristic of train. AIP Advances, 7(7) (2017) 075112. doi:10.1063/1.4995985.

[4]- L. Léger, E. Moreau, G. Artana, G. Touchard, Influence of a DC corona discharge on the airflow along an inclined flat plate. J. Electrostatics, 51-52 (2001) 300-306. doi:10.1016/S0304-3886(01)00089-4.

[5]- B. Dong, J.-M. Bauchire, J.M. Pouvesle, P. Magnier, D. Hong, Experimental study of a DBD surface discharge for the active control of subsonic airflow. J. Phys. D: Appl. Phys., 41 (2008) 155201 (9 pages). doi:10.1088/0022-3727/41/15/155201.

[6]- A. Soldati, S. Banerjee, Turbulence modification by large-scale organized electrohydrodynamic flows. Phys. Fluids, 10(7) (1998) 1742-1756. doi:10.1063/1.869691.

[7]- T. Yamamoto, Y. Morita, H. Fujishima, M. Okubo, Three-dimensional EHD simulation for point corona electrostatic precipitator based on laminar and turbulent models. J. Electrostatics, 64(7) (2006) 628-633. doi:10.1016/j.elstat.2005.10.015.

[8]- D. Semmar, J.M. Bauchire, D. Hong, N.A. Messaoudene, Descriptive numerical approach of the influence of an electrical discharge on a air flow. High Temperature Material Processes: An International Quarterly of High-

Technology Plasma Processes 12(1-2) (2008) 11-22. doi:10.1615/HighTempMatProc.v12.i1-2.20.

[9]- K. Mehalaine, D. Semmar, N.A. Messaoudene, J.M. Bauchire, D. Hong, Effects of corona discharges on a turbulent air flow: Simulation on a high-lift system. J. Electrostatics, 76 (2015) 171-177. doi:10.1016/j.elstat.2015.05.027.

[10]- P. Magnier. Experimental study of subsonic aerodynamic flow control by action of cold surface plasmas at atmospheric pressure - Etude expérimentale du contrôle d'écoulements aérodynamiques subsoniques par action de plasmas froids surfaciques à pression atmosphérique. Université d'Orléans, 2007.

[11]- E. Moreau, L. Léger, G. Touchard, Effect of a DC surface-corona discharge on a flat plate boundary layer for air flow velocity up to 25m/s. J. Electrostatics, 64(3) (2006) 215-225. doi:10.1016/j.elstat.2005.05.009.

[12]- H. Schlichting, K. Gersten, E. Krause, H.J. Oertel, C. Mayes, Boundary Layer Theory Springer. Eigth Revised and Enlarged Edition, (2000).

[13]- J.C. Matéo-Valez, F. Thivet, P. Degond, Elementary modeling of the ionic wind in a corona discharge, in 4th conference of the French electrostatics company Poitiers, France (2004).